

Preprocessors Matter! Realistic Decision-Based Attacks on Machine Learning Systems

Chawin Sitawarin^{1,2} Florian Tramer² Nicholas Carlini²
¹ University of California, Berkeley ² Google

Abstract—Decision-based adversarial attacks construct inputs that fool a machine learning model into making targeted mispredictions by making only hard-label queries. For the most part, these attacks have been applied directly to isolated neural network models. However, in practice, machine learning models are just a component of a much larger system. By adding just a *single* preprocessor in front of a classifier, we find that state-of-the-art query-based attacks are as much as *seven* times less effective at attacking a prediction pipeline than attacking the machine learning model alone. We explain this discrepancy by the fact that most preprocessors introduce some notion of *invariance* to the input space. Hence, attacks that are unaware of this invariance inevitably waste a large number of queries to re-discover or overcome it. We therefore develop techniques to first reverse-engineer the preprocessor and then use this extracted information to attack the end-to-end system. Our extraction method requires only a few hundreds queries to learn the preprocessors used by most publicly available model pipelines, and our preprocessor-aware attacks recover the same efficacy as just attacking the model alone. The code can be found at <https://github.com/google-research/preprocessor-aware-black-box-attack>.

I. INTRODUCTION

Machine learning is now widely used to secure systems that might be the target of evasion attacks, with perhaps the most common use being the detection of abusive, harmful or otherwise unsafe content [11, 19, 37]. When used in this way, it is critical that these systems are reliable in the presence of an adversary who seeks to evade them.

Worryingly, an extensive body of work has shown that an adversary can generate *adversarial examples* to fool machine learning models [3, 32]. The majority of these papers focuses on the *white-box* threat model: where an adversary is assumed to have perfect information about the entire machine learning model [7]. An adversary rarely has this access [34] in practice, and must instead resort to a *black-box* attack [9]. Recently, there has been a growing body of research under this black-box threat model. Even given just the model’s decision, it is possible to generate imperceptible adversarial examples with *decision-based* attacks [4] given only thousands of queries.

Much of this black-box line of work often focuses exclusively on fooling stand-alone machine learning models and ignoring any systems built around them. While it is known that machine learning systems can in principle be evaded with adversarial examples—and some black-box attacks have been demonstrated on production systems [17]—it is not yet well understood how these attacks perform on full systems compare to isolated models. In particular, this crucial distinction is rarely discussed by the papers proposing these new attacks.

We show that existing black-box attacks [5, 8, 10, 20] are significantly less effective when applied in practical scenarios as opposed to when they are applied directly to an isolated machine learning model. For example, under standard settings, an adversary can employ a decision-based attack to evade a standard ResNet image classifier with an average ℓ_2 -distortion of 3.7 (defined formally later). However, if we actually place this classifier as part of a full machine learning system, which has a preprocessor that trivially modifies the input (e.g., by resizing) before classification, the required distortion increases by **over a factor of seven** to 28.5! Even by tuning the hyperparameters or increasing the number of attack iterations, we can not completely resolve this issue (e.g., reducing the above distortion to just 16.5, still $4\times$ larger). Thus, we argue that existing black-box attacks have fundamental limitations that make them sub-optimal in practice.

To remedy this, we develop an improved attack that allows us to recover the original attack success rate even when attacking models with unknown preprocessors. Specifically, we combine methods from model extraction attacks and query-based attacks. Our attack begins by making a few queries to the system to determine any preprocessor used in the input pipeline (Section VII) and then uses the remaining queries to mount a (modified) version of the query attack (Section V and VI). Our extraction procedure is efficient and often requires only a few hundred queries to identify common preprocessing setups. As a result, at modest query budgets, it is more efficient to run our preprocessor extraction prior to mounting the attack than just blindly running any attack algorithm. In fact, we find that switching from a preprocessor-unaware attack to a preprocessor-aware attack is *more important* than switching from the worst to the best decision-based attack algorithm. Especially in settings where multiple images are to be attacked, the queries used for our one-time extraction procedure can be amortized across these multiple images.

In summary, we make the following contributions:

- 1) We quantify the degree to which query-based attacks are impacted by common image preprocessors, e.g., resizing, cropping, quantization, and compression;
- 2) We develop a query-efficient technique to reverse-engineer the preprocessor used by a remote system;
- 3) We use this stolen preprocessor to develop two improved versions of the attacks, *Bypassing and Biased-Gradient Attacks*, that recover the original attack efficacy even in the presence of preprocessors.

II. BACKGROUND AND RELATED WORK

A. Adversarial Examples

Adversarial examples [13, 32] are inputs designed to fool a machine learning classifier [3]. Typically, this is formalized by saying an example x has an adversarial example $x' = x + \delta$ if $f(x) \neq f(x')$ for some classifier f , where δ is a small perturbation under some ℓ_p -norm, i.e., $\|\delta\|_p \leq \epsilon$. Adversarial examples can be constructed either in the white-box setting (where the adversary uses gradient descent to produce the perturbation δ [7, 21]), or more realistically, in the black-box setting (where the adversary uses just query access to the system) [4, 9, 23]. Our paper focuses on this black-box setting with ℓ_2 -norm perturbations.

Adversarial examples need not always exploit the image classifier itself. For example, most machine learning models will resize an input image, e.g., from 1024×1024 to 224×224 pixels before actually classifying it. *Image scaling attacks* [26] take advantage of this property to construct a high-resolution image x so that after resizing to the smaller \hat{x} , the low resolution image will appear visually dissimilar to x . As a result, any accurate classifier will (correctly) classify the high-resolution image and the low-resolution image differently.

Query-Only Attacks. As mentioned above, an attacker can generate adversarial examples with only query access to the remote model. Unlike transferable adversarial examples which only succeed some of the time, query-based attacks succeed just as often as gradient-based attacks. Early query-only attacks perform gradient estimation [9], and then follow the gradient-based attacks. However, these attacks only work when given full probability outputs from a model.

A more practical category of query-based attack are *decision-based* attacks [4] which only use the arg-max label. These are the attacks we consider in this paper. At a high level, decision-based attacks generally work by first finding the decision boundary between the original image and the target label of interest, and then, by walking along the decision boundary, the total distortion can be slowly reduced until the image is misclassified. We study four decision-based attacks in this paper: Boundary, Sign-OPT, HopSkipJump (or HSJA), and QEBA [4, 8, 10, 20].

One well understood feature of black-box attacks is that they should operate at the lowest-dimensional input space possible. For example, AutoZOOM [36] improves on the simpler ZOO attack by constructing adversarial examples in a lower-dimensional embedding space, and SimBA [14] generates adversarial examples using low dimensional Fourier space. This phenomenon will help explain some of the results we observe when we find high-dimensional images require more queries than low-dimensional images.

B. Preprocessor Defense

Given an input x' that might be adversarial, there is an extensive literature on constructing defenses aiming to classify x' correctly. One large category of attempted defenses are those that preprocess inputs before classification [15, 31]. Unfortunately, these defenses are largely ineffective [2, 33], and improved attacks have found they do not improve the robustness above baseline undefended models.

However, surprisingly, recent work has shown that achieving robustness in the black-box setting is almost trivial. To prevent current query attacks from succeeding, it suffices to transform images by adding an almost-imperceptible amounts of noise to the image [1, 25]. This suggests that there may be a significant gap between the capabilities of white- and black-box attacks when preprocessors are present.

C. Model Stealing Attacks

In order to improve the efficacy of black-box attacks, we will make use of various techniques from the model stealing literature [35]. This research direction asks the question: given query access to a remote machine learning model, can we reverse-engineer how it works? Attacks are typically evaluated based on their *accuracy* (i.e., how well the stolen model works on the test data) and their *fidelity* (i.e., how closely the stolen model mirrors the predictions of the original model) [18]. Because we intend to use model stealing to better attack a remote system, we do not care much about how well the attack does on the test data, but rather how well attacks will *transfer* between the stolen and original model—which means we want high fidelity. Specifically, we extend a recent line of work that shows how to achieve functional equivalence [6, 22, 28], and we leverage ideas from this space to recover the exact preprocessor used by a remote machine learning model.

III. SETUP AND THREAT MODEL

A. Notation

We denote an unperturbed input image in the *original space* as $x_o \in \mathcal{X}_o := [0, 1]^{s_o \times s_o}$ and a processed image in the *model space* as $x_m \in \mathcal{X}_m \subseteq [0, 1]^{s_m \times s_m}$. The original size s_o can be the same or different from the target size s_m . A preprocessor $t : \mathcal{X}_o \rightarrow \mathcal{X}_m$ maps x_o to x_m , i.e., $x_m = t(x_o)$. For instance, a resizing preprocessor that maps an image of size 256×256 pixels to 224×224 pixels means that $s_o = 256$, $s_m = 224$, and $\mathcal{X}_m = [0, 1]^{224 \times 224}$. As another example, an 8-bit quantization restricts \mathcal{X}_m to a discrete space of $\{0, 1/255, 2/255, \dots, 1\}^{s_m \times s_m}$ and $s_o = s_m$.

The classifier, excluding the preprocessor, is represented by a function $f : \mathcal{X}_m \rightarrow \mathcal{Y}$. The label space, \mathcal{Y} , is a set of all possible labels $\{1, 2, \dots, Y\}$. Finally, the entire classification pipeline is denoted by $f \circ t : \mathcal{X}_o \rightarrow \mathcal{Y}$.

B. Threat Model

We focus on the common test-time evasion attack where the adversary has no control over the system other than the ability to modify inputs to the model. The adversary’s goal is to minimally perturb the input such that it is misclassified by the victim classifier.

The key distinguishing factor between our work and previous works is that we allow for the existence of a *preprocessing pipeline as part of the victim system*. In other words, the adversary cannot simply run an attack algorithm on the model input space which is often oversimplified. That is, we follow in the direction of Pierazzi et al. [24] and develop attacks that work end-to-end, as opposed to just attacking the model alone. To do this we will develop strategies to “bypass” the preprocessors (Section V and VI) and to find out which

preprocessors are being used in the first place (Section VII). Common preprocessors used in deployed systems include resizing, quantization, and image compression, for example.

While existing query-based attacks can still work in the presence of an unknown preprocessing stage, *we show that not taking the preprocessing into account makes all previously proposed attacks significantly (up to 7×) less effective.* Our methods, assuming that the preprocessor is known, recover this lost efficiency. In particular, we consider the following threat model:

- We consider a *black-box query-based* adversary, meaning that the adversary can query the victim model with any input and observe the corresponding *hard-label* output but know nothing else about the system. The adversary has a limited query budget per input.
- The adversary wants to misclassify as many perturbed inputs as possible, while minimizing the perturbation size—measured by Euclidean distance (ℓ_2 -norm) in *the original input space*, \mathcal{X}_o .
- We assume the victim system accepts inputs of any dimension, and the desired model input size is obtained by cropping and resizing as part of a preprocessing pipeline (as most image-based services do).
- We consider both targeted and untargeted attacks; but place a stronger emphasis on the former.

C. Experiment Setup

Similarly to previous works [4], we evaluate our attacks on a classifier (ResNet-18 [16]) trained on the ImageNet dataset [12]. We use a pretrained model from a well-known repository `timm` [38] which is implemented in PyTorch and trained on inputs of size 224×224 . This model is fixed throughout all the experiments. We consider four different attack algorithms in total, Boundary Attack [4], Sign-OPT Attack [10], HopSkipJump Attack (HJSA) [8], and QEBA [20]. The first three attacks have both targeted and untargeted versions while QEBA is only used as a targeted attack.

Implementations of Boundary Attack and HSJA are taken from the `FOOLBOX` package [27].¹ For Sign-OPT Attack and QEBA, we use the official, publicly available implementation.² We also observe that choices of hyperparameters of each attack algorithm substantially affect its performance and that the default ones do not work well when a preprocessor is applied. As such, we combine a hyperparameter sweep into the attack and report results with both the best and the default set of hyperparameters. This emphasizes how knowledge of the preprocessor not only affects the attack algorithm itself but also how the hyperparameters are chosen.

We find that the choice of hyperparameters of the four attack algorithms play an important role in their effectiveness, and it is not clear how an attacker would know apriori how to choose such hyperparameters. In reality, the adversary would benefit from spending some queries to tune the hyperparameters on a few samples. Coming up with the most efficient tuning algorithm is outside of the scope of this work. Nonetheless,

¹We use code from the commit: <https://github.com/bethgelab/foolbox/commit/de48acaaf46c9d5d4ea85360cadb5ab522de53bc>.

²Sign-OPT attack: <https://github.com/cmhcbb/attackbox>. QEBA: <https://github.com/AI-secure/QEBA>.

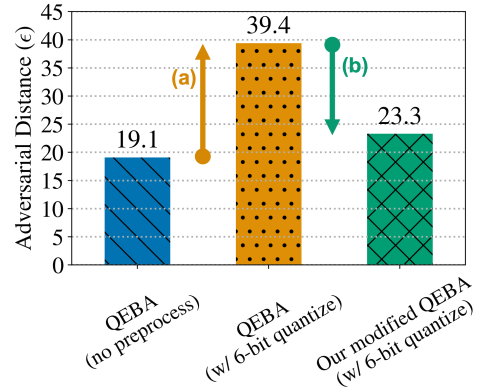


Fig. 1: Unmodified query-based attacks perform much worse when there is an input preprocessor in front of a classifier, i.e., it finds adversarial examples with a significantly higher adversarial distance ϵ compared to the same attack but without the preprocessor (39.4 vs 19.1 or arrow (a)). Conversely, our attack utilizes the knowledge of the preprocessor and almost completely recovers, as shown by arrow (b), the missing efficacy (23.3 vs 19.1).

we account for this effect by repeating all experiments with multiple choices of hyperparameters and reporting the results with both the default and the best sets in Section V-C and VI-C. We further discuss some common trends in Section VIII-B, and the detail of our experiments is included in Appendix A.

To compare effectiveness of the attacks, we report the average perturbation size (ℓ_2 -norm) of the adversarial examples computed on 1,000 random test samples. We will refer to this quantity as the adversarial distance in short. Smaller adversarial distance means a stronger attack. Unless stated otherwise, all the attacks use 5,000 queries per one test sample.

IV. PREPROCESSORS MATTER

We begin by quantifying the degree to which an adversary could benefit by having knowledge of the preprocessor. We follow the experimental setup defined above, using a ImageNet-trained classifier either as-is, or with a preprocessor that quantizes images to six bits.

Attacks perform worse with preprocessors. To illustrate how poorly the preprocessor-oblivious attack can perform, we will use the current state-of-the-art targeted query-based attack, QEBA [20]. We consider two adversaries: (1) QEBA with default hyperparameters on a classifier without any preprocessor, and (2) QEBA with default hyperparameters on the same classifier with 6-bit quantization preprocessor. The outcome is shown in Fig. 1 where adversary (1) finds the mean adversarial distance of 19.1 while adversary (2) finds a much larger distance of 39.4, more than a $2\times$ increase. Fig. 2 visually compares the adversarial examples generated by these two adversaries.

Are preprocessors just more adversarially robust? The above observation that it requires more queries to attack a defense with a preprocessor has two possible explanations:

- 1) decision-based attacks performs sub-optimally when there is a preprocessor present; or,



(a) Original Samples



(b) Unaware Attack's Adversarial Examples



(c) Our Biased-Gradient Attack's Adversarial Examples

Fig. 2: The adversarial examples generated by (b) the preprocessor-unaware attack have more perceptible perturbation (larger ℓ_2 -norm) compared to ones from (c) our Biased-Gradient Attack. These four samples are randomly chosen from the test set of ImageNet, and both of the attacks are based on QEBA.

- 2) placing a preprocessor in front of a model makes it truly more robust to adversarial examples.

However, it is well known that quantization input preprocessor does not improve adversarial robustness [7]—even in the case of Guo et al. [15] who performs significant quantization [2]. Therefore, it is likely that QEBA is performing poorly. Also, the underlying cause is not related gradient obfuscation [2] as QEBA is a decision-based attack and does not utilize the gradients.

More queries are insufficient to recover effectiveness. One final possibility remains. It is possible that placing a preprocessor in front of a model makes it more query-inefficient to attack. Then, decision-based attacks might eventually recover the same quality of adversarial examples when run with sufficient query budget. We find that this is not the case: the mean adversarial distance on the classifier with quantization plateaus at 31.9, still 50% higher than the one without. This experiment will be discussed further in Section VIII-A.

Our improved attack solves the issue. Knowing which preprocessors are used in the target system significantly improves the efficiency of the attacks as shown by the right green bar in Fig. 1. In Section V and Section VI, we describe our improved attacks which remain effective in the presence of preprocessors. But this begs the question: is it actually possible for an adversary to know what preprocessor is being used? In Section VII, we will show that this knowledge can be easily extracted in a few hundred (decision-only) queries to the black-box machine learning system.

V. PREPROCESSOR BYPASSING ATTACK

Given that even simple preprocessing of the input causes a degradation of attack efficacy, we now develop approaches to counteract this effect. For now, we assume the adversary is aware of the preprocessing function being applied, and in Section VII, we will introduce techniques that can efficiently extract this information.

Why should preprocessor knowledge help the adversary?

We see two intuitive reasons to believe this. First, as discussed above, we know that preprocessors do not improve the white-box robustness, and so it is unlikely that they improve the black-box robustness. Second, in the limit, an adversary who performs a complete functionally-equivalent model extraction attack [18] would be able to mount a query-only attack with zero queries—because they would have a perfect local copy of the model. Our intuition here is that while performing a full model extraction attack might be incredibly costly, it might be possible to spend just a few up-front queries to steal the preprocessor, and then use this knowledge to generate attacks much more efficiently.

We develop two attack algorithms that are effective on different types of preprocessors. The first is *Bypassing Attack*, discussed here (the second, Biased-Gradient Attack, will be discussed in the next section). The intuition behind our attack is that most input preprocessing wastes the attacker's queries or reduces the amount of knowledge that can be revealed by these queries. So we design our Bypassing Attack to generate queries that “bypass” the preprocessor.

Invariance wastes attack queries. Generally, attack algorithms either query a model to gain additional information about the victim model (e.g., to approximate the gradient) or query a model to perturb the input and move it closer to the decision boundary. Since most preprocessors are not injective functions, many perturbations made in the original input space will map onto the same processed image. In other words, preprocessing makes the model's output *invariant* to some specific perturbations. This prevents the attack from gaining new information about the model with the query and might actually deceive themselves into thinking they have learned something incorrect. We note that the effect of the invariance also depends on the ℓ_p -norm of the attack. For instance, ℓ_2 -norm attacks may struggle against a cropping preprocessor, but ℓ_∞ -norm attacks should not.

Our bypassing Attack. Exploiting knowledge of the preprocessor, our Bypassing Attack creates queries that avoid the invariances by circumventing the preprocessor completely. Briefly, our attack works by, *only querying the target pipeline with images that are already preprocessed so the actual preprocessor does not affect these inputs in any way*. Naturally, not all preprocessing functions can be bypassed. Our Bypassing Attack assumes (i) the preprocessors are *idempotent*, i.e., $t(t(x)) = t(x)$, and (ii) the preprocessor's output space is continuous. While these assumptions may sound unrealistically restrictive, two of the most common preprocessing functions—cropping and resizing—satisfy these properties. In fact, most of the common preprocessing functions are idempotent: for example quantizing an already quantized image. For preprocessors that do not satisfy Assumption (ii), e.g., quantization whose

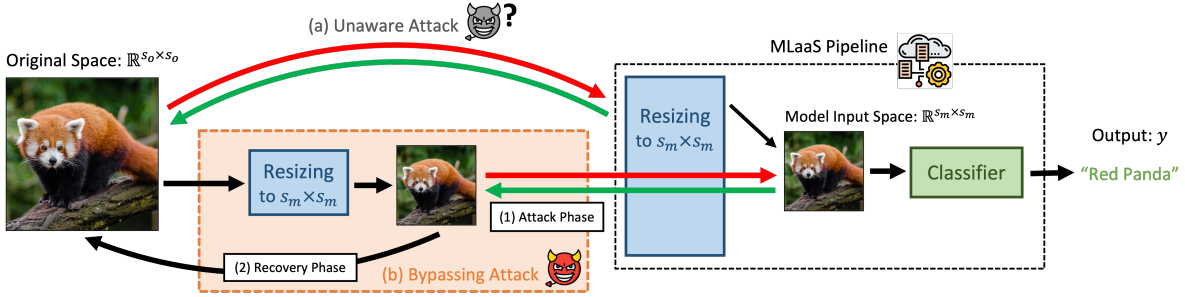


Fig. 3: Illustration of our Bypassing Attack with resizing as the preprocessor as a comparison to the unaware or preprocessor-oblivious attack. The red and the green arrows denote the query submitted by the attack and the output returned by the MLaaS pipeline, respectively. The attack phase of our Bypassing Attack first resizes the input image to the correct size used by the target pipeline. This allows any attack algorithm to operate on the model input space directly. The recovery phase then finds the adversarial example in the original space that maps to the one found during the attack phase.

output space is discrete, we propose an alternative, Biased-Gradient Attack, described in Section VI.

Fig. 3 conceptually depicts our attack idea. To allow the Bypassing Attack to query the model directly, we use knowledge of the preprocessor to first map the input image to the preprocessed space. Then, we execute the full decision-based attack directly on this preprocessed image. Finally, after we complete the attack, we recover the adversarial image in the original space.

More specifically, Bypassing Attack can be generally described as two phases: an attack phase and a recovery phase.

- 1) **Attack Phase:** The adversary runs any query-based attack algorithm as usual with no modification on the attack algorithm itself.
- 2) **Recovery Phase:** Once an adversarial example is obtained, the adversary has to convert it back to the original space.

Algorithm 1 shows a pseudocode of our Bypassing Attack combined with any attack algorithm that relies on gradient approximation, e.g., HSJA, QEBA. Bypassing Attack requires a simple initialization which projects a given input image to the model space before the attack phase.

With the threat model defined in Section III-B, the recovery phase aims to find an adversarial example with the minimum perturbation in the original space, given a successful adversarial example in the model space, x_m^{adv} , obtained from the attack phase. More formally, the recovery phase can be represented as the following optimization problem,

$$\arg \min_{z_o \in \mathcal{X}_o} \|z_o - x_o\|_2^2 \quad (1)$$

$$\text{s.t. } t(z_o) = x_m^{\text{adv}}. \quad (2)$$

For our Bypassing Attack, we will not explicitly optimize the problem solution. Rather, we will use a simple preprocessor-dependent technique to obtain the solution in closed form.

A. Cropping

Because almost all image classifiers operate on square images [38], one of the most common preprocessing operations

Input : Image x , label y , classifier f , preprocessor t
Output: Adversarial examples x^{adv}

```

1 // Initialization
2  $x' \leftarrow t(x)$ ;
3 // Attack Phase: run an attack
  algorithm of choice as usual
4 for  $i \leftarrow 1$  to  $num\_steps$  do
5    $\tilde{X} \leftarrow \{x' + \alpha u_b\}_{b=1}^B$  where  $u_b \sim \mathcal{U}$ ;
6    $\nabla_x S \leftarrow \text{ApproxGrad}(f \circ t, \tilde{X}, y)$ ;
7    $x' \leftarrow \text{AttackUpdate}(x', \nabla_x S)$ ;
8 end
9 // Recovery Phase: exactly recover
   $x^{\text{adv}}$  in original input space
10  $x^{\text{adv}} \leftarrow \text{ExactRecovery}(t, x')$ ;

```

Algorithm 1: Outline of Bypassing Attack. This example is built on top of gradient-approximation-based attack algorithm (e.g., HSJA, QEBA), but it is compatible with any of black-box attack. \mathcal{U} is distribution of vectors on a uniform unit sphere.

is to first crop the image to a square. In practice, this means that any pixels on the edge of the image are completely ignored by the classifier. As a result, there is no gradient with respect to these pixels, and outputs of the classifier are guaranteed to be invariant to any perturbation on these pixels.

An attacker who tries to perturb the edge pixels or to estimate gradients on them would inevitably waste queries. Yet, unless we actively tell the adversary this fact, the decision-based attack will need to figure this out for itself. Without this prior knowledge, it will need to re-discover that the pixels on the edge do not affect the prediction **for each and every pixel, one after the other**, potentially wasting tens of thousands of queries. On the other hand, with knowledge of the preprocessor, the attacker would be better off to just constrain the perturbation on the center pixels which are not ignored. This is exactly what the Bypassing Attack does. Precisely, the attack consists of the two following steps.

a) Attack Phase for Cropping: To bypass the cropping transformation, the attacker simply submits an already cropped

input and runs any query-based attack algorithm in the space $\mathbb{R}^{s_m \times s_m}$ instead of $\mathbb{R}^{s_o \times s_o}$. Without any modification on the attack algorithm, it is able to operate directly on the model space as if there is no preprocessing.

b) Recovery Phase for Cropping: In order for the adversarial example obtained from the attack phase to be useful in input-space, the adversary still has to produce an adversarial example in the original space with the smallest possible Euclidean distance to the original input. It should be obvious that for cropping, this operation simply equates to padding this adversarial example with the original edge pixels. For a more formal proof, see Appendix B.

B. Resizing

Resizing is, in practice, even more common than cropping. Because nearly all image classifiers require images to be of a specific size, every image that is not already of the correct size will generally be resized to one. Resizing is also preferable to cropping since it does not risk losing localized information on the edge of the image completely.

Not all image resizing operations are the same; the main step that varies between them is called the ‘‘interpolation’’ mode. Interpolation determines how the new pixels in the resized image depend on (multiple) pixels in the original image. Generally, resizing represents some form of a weighted average. How the weights are computed and how many of the original pixels should be used varies by specific interpolation methods.

Consider for the moment the special case of resizing an image with ‘‘nearest-neighbor interpolation’’, the simplest resizing operation. Conceptually, a nearest-neighbor interpolating resize operation is nearly identical to cropping. However, instead of cropping out all pixels on the edge of the image, nearest-neighbor resizing selects only 1 out of k pixels for each block of pixels. As a result, the intuition behind why knowledge of the preprocessor helps is the same: A naive attack algorithm that operates on the original space inevitably wastes a perturbation and queries on pixels that will never make their way past the preprocessor.

For other interpolation or resampling methods, e.g., bilinear, bicubic, the attack methodology is similar, but somewhat more involved mathematically. It turns out that, similarly to cropping, resizing is also a linear transformation for any of these three resampling methods. For $s_o > s_1$, we have that

$$x_m = t^{\text{res}}(x_o) = M^{\text{res}}x_o \quad (3)$$

For nearest interpolation (zeroth order), M^{res} is a sparse binary matrix with exactly one 1 per row. For higher-order interpolations, a pixel in x_m can be regarded as a weighted average of certain pixels in x_o . Here, M^{res} is no longer binary, and each of its rows represents these weights which are between 0 and 1. For instance, since one pixel in a bilinear resized image is a weighted average of four pixels (2×2 pixels) in the original image, M^{res} for bilinear interpolation has four non-zero elements per row. On the other hand, M^{res} for bicubic interpolation has 16 non-zero elements per row (4×4 pixels). M^{res} is still generally sparse for $s_o > s_1$ and is more sparse when s_o/s_1 increases.

The matrix M^{res} can be computed analytically for any given s_o and s_1 . Alternatively, it can be populated programmatically, by setting each pixel in the original image to 1, one at a time, then performing the resize, and gathering the output. This method is computationally more expensive but simple, applicable to any sampling order, and robust to minor differences in different resizing implementations.

a) Attack Phase for Resizing: The attack phase for resizing is exactly the same as that of cropping. The adversary simply runs an attack algorithm of their choice on the model space \mathcal{X}_m . The main difference comes in the recovery phase below.

b) Recovery Phase for Resizing: The recovery phase involves some amount of linear algebra, as it is equivalent to solving the following linear system of equations

$$x_m^{\text{adv}} = M^{\text{res}}x_o^{\text{adv}}. \quad (4)$$

to find x_o^{adv} . Note that for $s_o > s_m$, this is an underdetermined system so there exist multiple solutions. A minimum-norm solution, x_o^* , can be obtained by computing the right pseudo-inverse of M^{res} given by

$$(M^{\text{res}})^+ = (M^{\text{res}})^{\top} (M^{\text{res}}(M^{\text{res}})^{\top})^{-1} \quad (5)$$

$$x_o^* = (M^{\text{res}})^+ x_m^{\text{adv}} \quad (6)$$

However, the adversary does not want to find a minimum-norm original sample x_o^* but rather a minimum-norm perturbation $\delta_o^* = x_o^{\text{adv}} - x_o$. This can be accomplished by modifying Eqn. (4) and Eqn. (6) slightly

$$M^{\text{res}}(x_o + \delta_o^*) = x_m^{\text{adv}} \quad (7)$$

$$M^{\text{res}}\delta_o^* = x_m^{\text{adv}} - M^{\text{res}}x_o \quad (8)$$

$$\delta_o^* = (M^{\text{res}})^+ (x_m^{\text{adv}} - M^{\text{res}}x_o) \quad (9)$$

$$\delta_o^* = (M^{\text{res}})^+ (x_m^{\text{adv}} - x_m). \quad (10)$$

Eqn. (10) summarizes the recovery phase for resizing. By construction, it guarantees that δ_o^* is a minimum-norm perturbation for a given x_m^{adv} , or $x_o^{\text{adv}} = x_o + \delta_o^*$ is a projection of x_o onto the set of solutions that map to x_m^{adv} after resizing. In other words, by replacing any δ_o with $z_o - x_o$, we have

$$x_o^{\text{adv}} = \arg \min_{z_o \in \mathbb{R}^{s_o \times s_o}} \|z_o - x_o\|_2 \quad (11)$$

$$\text{s.t. } M^{\text{res}}z_o = x_m^{\text{adv}}. \quad (12)$$

In practice, we can compute δ_o^* by either using an iterative solver on Eqn. (4) directly, or by pre-computing the pseudo-inverse in Eqn. (5). The former does not require caching any matrix but must be recomputed for every input. Caching the pseudo-inverse is more computationally expensive but is done only once. Since M^{res} is sparse, both options are very efficient.

C. Bypassing Attack Results

a) Model without preprocessors: First, we run the attacks on the standard victim model without any preprocessing. The results in Table I confirm the prior conclusion that HSJA performs best among untargeted attacks and QEBA is the best among targeted attacks. Apart from Boundary Attack, the default hyperparameters are often the best or very close

TABLE I: Comparison of the mean adversarial distortion among all attacks with both best and default hyperparameters. When the default hyperparameters are also the best, we report the same result in both columns.

Attack Objectives	Attacks	Default	Best
Untargeted	Boundary	9.5	4.6
	Sign-OPT	5.7	5.7
	HSJA	3.8	3.6
Targeted	Boundary	41.6	36.7
	Sign-OPT	45.6	45.6
	HSJA	34.0	32.2
	QEBA	19.1	19.1

to the best ones. We will refer to this table to compare how simple and common preprocessors make the attacks much less effective.

b) Cropping: Now we consider a common cropping operation that center crops an image of size 256×256 pixels down to 224×224 pixels, i.e., $s_o = 256, s_m = 224$. Table II reports the mean adversarial distance when the attacks are run without taking the preprocessor into account (“Unaware”) and when they are run as part of our Bypassing Attack. For all attack algorithms and for both the default and the best hyperparameters, the Bypassing version outperforms the normal one that is unaware of the preprocessor. The adversarial distance found by the baseline is about 8–16% higher than that of the Bypassing Attack counterpart for both targeted and untargeted settings. We note that this number is very close to the ratio between a square root of the ratio between the number of pixels in the full image and in the cropped image: $\sqrt{256^2/224^2} \approx 1.14$. This difference is exactly the portion of the border pixels that are cropped out which suggests that the attacks without the Bypassing mechanism do waste perturbation on these invariant pixels.

We also observe that the mean adversarial distance of our Bypassing Attack is very close to the adversarial distance when there is no preprocessor as shown in Table I earlier. This should be expected because the Bypassing Attack for cropping operates in $[0, 1]^{224 \times 224}$, the same as the no-preprocessor case, and by design, it wastes no perturbation on the border pixels.

c) Resizing: For resizing, we study the three most common interpolation or resampling techniques, i.e., nearest, bilinear, and bicubic. The results are shown in Table III, IV, and V, respectively. The improvement from the Bypassing Attack is proportional to the original input dimension. For an input size of 1024×1024 , a reasonable image size captured by digital or phone cameras, **our attack reduces the mean adversarial distance by up to $4.6 \times$ compared to the preprocessor-oblivious counterpart.**

We emphasize that our Bypassing Attack finds adversarial examples with about the same mean adversarial distance as the no-preprocessor case **regardless of the input dimension**. This is illustrated in Fig. 4. This may seem counter-intuitive: one might expect that the ℓ_2 -norm of the adversarial perturbation scales with the square root of the input dimension. This may be the case if a new classifier were trained on each of the different input sizes [29]. But here, the neural network is *fixed*, and the resizing operation “throws away” some of the pixels.

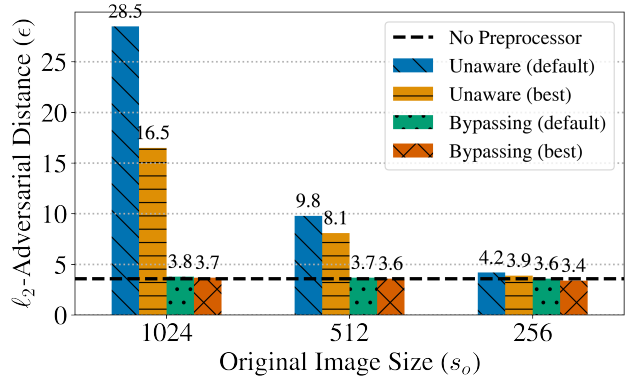


Fig. 4: Preprocessor-unaware attacks have a challenging time effectively generating adversarial examples. By re-tuning attack hyperparameters (“default”→“best”) unaware attacks can be improved somewhat, but by applying our Bypassing Attack we can generate adversarial examples nearly as effectively as if no preprocessor was present at all. Here, the preprocessor is resizing with nearest interpolation from varying sizes to 224×224 , and the attack algorithm is untargeted HSJA. The dashed line indicates the adversarial distance found by the same attack when no preprocessor is used.

To explain this phenomenon, let’s consider a toy example of a binary classifier that simply classifies one-dimensional data, e.g., white and black pixels with values of 0 and 1 respectively, by using a 0.5 threshold. To push a white pixel over the decision boundary (or the threshold, in this case) requires a perturbation of size 0.5. Now consider a new set of inputs with size 2×2 and a nearest resize that maps the 2×2 inputs to one pixel. The classifier remains unchanged. In this case, the nearest resize simply picks one pixel (say, the top left) out of the four pixels. Which pixel is picked depends on the exact implementation but does not matter for our purpose here. To attack this classifier from a 2×2 input, the adversary still needs to change only the top left pixel by 0.5, and thus, the adversarial distance remains unchanged. Even for larger input sizes, only one pixel will still be selected. While this toy example explains resizing with nearest interpolation, it does not necessarily apply to bilinear or bicubic. Nonetheless, all of our experimental results support this hypothesis.

The factor of improvement scales with a square root of the size of the original dimension, similarly to cropping. For example, when the original input size goes from 1024×1024 to 512×512 , we can expect the improvement on the mean adversarial distance to be cut by about half. This is due to (1) the earlier observation that our Bypassing Attack is mostly agnostic to the original input dimension and (2) the fact that the adversarial distance found by the baseline attacks does scale with a square root of the dimension.

Consequently, when the original input size is sufficiently large (above 256×256 in our setting), the Bypassing Attack is always preferable to the resizing-oblivious attack both with and without hyperparameter tuning. On the other hand, when the original and the model input sizes are very close, the benefits of our Bypassing Attack diminish. This is because the attack algorithm in Bypassing Attack operates in the model space

TABLE II: Comparing the mean adversarial perturbation norm for cropping. The numbers in the parentheses indicate s_o and s_m , respectively. ‘‘Change’’ is a ratio between the perturbation norm under a preprocessor-unaware (‘‘Unaware’’) vs our Bypassing Attack, both using their respectively best set of hyperparameters. The smallest adversarial distance found with untargeted and targeted attacks is in bold. For the distance, lower is better.

Preprocessors	Methods	Hparams	Untargeted Attacks			Targeted Attacks			
			Boundary	Sign-OPT	HSJA	Boundary	Sign-OPT	HSJA	QEBA
Crop (256 \rightarrow 224)	Unaware	Default	11.1	6.7	4.4	48.6	50.6	40.9	24.7
		Best	5.3	6.5	4.2	42.8	50.4	38.2	22.2
	Bypassing (ours)	Default	9.6	5.9	3.9	42.3	46.0	35.1	21.2
		Best	4.6	5.8	3.6	37.3	46.0	32.9	19.6
		Change	1.16 \times	1.12 \times	1.16 \times	1.15 \times	1.08 \times	1.16 \times	1.13 \times

TABLE III: Comparing the mean adversarial perturbation norm for resizing with *nearest-neighbor* resampling. The values in the left column denote the original and final size with ($s_o \rightarrow s_m$).

Preprocessors	Methods	Hparams	Untargeted Attacks			Targeted Attacks			
			Boundary	Sign-OPT	HSJA	Boundary	Sign-OPT	HSJA	QEBA
Resize (1024 \rightarrow 224) (Nearest)	Unaware	Default	45.4	24.8	28.5	194.4	201.3	168.3	124.5
		Best	21.2	24.8	16.5	172.2	198.8	153.4	90.5
	Bypassing (ours)	Default	9.8	5.8	3.8	42.3	46.3	35.2	19.4
		Best	4.7	5.8	3.7	37.7	46.3	33.3	19.4
	Change	4.49 \times	4.31 \times	4.56 \times	4.57 \times	4.30 \times	4.61 \times	4.67 \times	
Resize (512 \rightarrow 224) (Nearest)	Unaware	Default	22.4	12.5	9.8	95.5	97.8	79.5	51.2
		Best	10.3	12.5	8.1	84.7	97.8	74.2	44.5
	Bypassing (ours)	Default	9.5	5.8	3.8	41.6	98.0	35.1	19.4
		Best	4.5	5.7	3.6	37.3	45.5	32.6	19.4
	Change	2.27 \times	2.20 \times	2.24 \times	2.27 \times	2.15 \times	2.28 \times	2.30 \times	
Resize (256 \rightarrow 224) (Nearest)	Unaware	Default	10.6	6.3	4.2	46.5	50.6	38.6	20.3
		Best	6.3	6.1	3.9	41.0	50.6	36.1	20.1
	Bypassing (ours)	Default	9.2	5.4	3.6	40.7	45.1	33.2	17.9
		Best	7.7	5.4	3.4	36.0	44.8	31.3	17.9
	Change	0.82 \times	1.13 \times	1.13 \times	1.14 \times	1.13 \times	1.15 \times	1.13 \times	

and hence, minimizes the adversarial distance in that space, i.e., the distance between x_m^{adv} and $x_m = t(x_o)$. This distance is likely correlated but not necessarily the same as the true objective distance, which is measured in the original space, i.e., the distance between x_o^{adv} and x_o . Hence, when s_o and s_m are close, the downside of this objective mismatch outweighs the benefit of the bypassing mechanism.

VI. BIASED-GRADIENT ATTACKS

We now turn our attention to more general preprocessors that cannot be bypassed without modifying the search space in a major way. The first example of these preprocessors is quantization which turns the continuous space into a discrete space. In practice, 8-bit quantization is automatically applied as pixel values are represented as an integer in the range $[0, 255]$. However, most of the prior black-box attacks ignore this fact and operates on the continuous domain. Bypassing quantization means that an attack algorithm has to search for adversarial examples in the discrete space which is much more difficult and incompatible with the majority of the black-box attacks. Another example is JPEG compression, a popular image compression algorithm involving splitting an image into multiple patches and then discretizes the frequency space. It is no longer obvious how to efficiently search in the output space of JPEG compression while also trying to minimize the perturbation in the original space.

Input : Image x , label y , classifier f , preprocessor t
Output: Adversarial examples x^{adv}

```

1 // No special initialization
2  $x' \leftarrow x$ ;
3 // Attack Phase: run modified attack
4 for  $i \leftarrow 1$  to  $num\_steps$  do
5   // Biased gradient approximation
6    $\tilde{X} \leftarrow \{t(x' + \alpha u_b)\}_{b=1}^B$  where  $u_b \sim \mathcal{U}$ ;
7    $\bar{\nabla}_{t(x)} S \leftarrow \text{ApproxGrad}(f \circ t, \tilde{X}, y)$ ;
8   // Backprop gradients through  $t$ 
9    $\bar{\nabla}_x S \leftarrow \text{BackProp}(\bar{\nabla}_{t(x)} S, t)$ ;
10   $x' \leftarrow \text{AttackUpdate}(x', \bar{\nabla}_x S)$ ;
11 end
12 // Recovery Phase: optimization-based
   recover  $x^{\text{adv}}$  in original space
13  $x^{\text{adv}} \leftarrow \text{OptRecovery}(t, x')$ ;
```

Algorithm 2: Outline of Biased-Gradient Attack built on top of gradient-approximation-based attack algorithm (e.g., HSJA, QEBA). \mathcal{U} is distribution of vectors on a uniform unit sphere.

For this type of preprocessors, we propose the Biased-Gradient Attack which, unlike Bypassing Attack, operates in the original space. Instead of applying a black-box attack

TABLE IV: Comparing the mean adversarial perturbation norm for *bilinear* resizing.

Preprocessors	Methods	Hparams	Untargeted Attacks			Targeted Attacks			
			Boundary	Sign-OPT	HSJA	Boundary	Sign-OPT	HSJA	QEBA
Resize (1024 → 224) (Bilinear)	Unaware	Default	66.0	38.2	43.6	217.9	213.5	202.0	125.4
		Best	32.7	38.2	25.5	198.3	213.0	188.4	90.3
	Bypassing (ours)	Default	15.6	9.4	6.3	65.3	70.9	53.9	30.0
		Best	7.4	9.1	6.0	58.2	70.9	50.3	30.0
		Change	4.40×	4.18×	4.26×	3.41×	3.01×	3.74×	3.01×
	Resize (512 → 224) (Bilinear)	Unaware	Default	32.0	19.1	15.2	107.7	106.4	96.2
Best			15.9	19.1	12.6	98.7	106.0	90.8	45.6
Bypassing (ours)		Default	15.4	9.3	6.2	65.3	70.9	53.5	30.3
		Best	7.4	9.2	5.9	57.7	70.9	50.2	30.3
		Change	2.16×	2.07×	2.14×	1.71×	1.50×	1.81×	1.51×
Resize (256 → 224) (Bilinear)		Unaware	Default	13.2	7.8	7.3	50.7	53.0	42.3
	Best		6.3	7.8	5.1	45.6	53.0	40.8	21.9
	Bypassing (ours)	Default	14.6	10.0	8.2	49.8	58.1	48.0	21.5
		Best	7.7	9.9	6.1	45.5	57.8	46.2	21.5
		Change	0.82×	0.79×	0.83×	1.00×	0.92×	0.88×	1.02×

TABLE V: Comparing the mean adversarial perturbation norm for *bicubic* resizing.

Preprocessors	Methods	Hparams	Untargeted Attacks			Targeted Attacks			
			Boundary	Sign-OPT	HSJA	Boundary	Sign-OPT	HSJA	QEBA
Resize (1024 → 224) (Bicubic)	Unaware	Default	52.8	29.2	34.2	206.6	207.3	181.7	127.7
		Best	25.7	29.2	20.6	184.8	207.3	171.6	91.2
	Bypassing (ours)	Default	11.9	7.3	4.9	53.2	58.0	43.0	23.8
		Best	5.8	7.1	4.5	46.4	57.7	40.6	23.8
		Change	4.44×	4.10×	4.54×	3.96×	3.59×	4.23×	3.83×
	Resize (512 → 224) (Bicubic)	Unaware	Default	26.8	15.5	12.1	101.4	102.1	85.7
Best			13.1	15.4	10.1	91.1	101.5	81.1	44.3
Bypassing (ours)		Default	12.1	7.1	4.7	52.2	56.8	42.1	24.4
		Best	5.8	7.0	4.5	46.4	56.6	40.2	24.4
		Change	2.28×	2.19×	2.25×	1.96×	1.79×	2.02×	1.82×
Resize (256 → 224) (Bicubic)		Unaware	Default	12.5	7.6	5.1	49.5	51.9	41.5
	Best		6.0	7.4	4.8	44.2	51.9	39.4	21.5
	Bypassing (ours)	Default	11.7	7.4	4.9	48.2	53.3	39.2	21.6
		Best	5.8	7.3	4.6	42.5	52.9	37.6	21.6
		Change	1.04×	1.01×	1.03×	1.04×	0.98×	1.05×	1.00×

algorithm as is, the Biased-Gradient Attack modifies the base attack in order to bias the perturbation toward directions that the preprocessor is more sensitive to. The intuition is that while it is difficult to completely avoid the invariance of the preprocessor, we can encourage the attack to explore directions that will result in a larger change in the output space of the preprocessing function.

Our Biased-Gradient Attack still consists of the attack and the recovery phases. Fig. 5 shows a simple diagram of the Biased-Gradient Attack on quantization as a preprocessor, and Algorithm 2 summarizes it as a pseudocode. Since the Biased-Gradient Attack is general and not specific to a preprocessor, we will describe the attack and the recovery phases independently of a specific preprocessing function.

A. Attack Phase

We utilize the preprocessor knowledge to modify the base attack algorithm in two ways. In particular, we focus on attacks with gradient approximation like HSJA and QEBA since they perform consistently better than the others.

Biased Gradient Approximation We modify the gradient approximation step to account for the preprocessor. First, consider the adversary’s loss function defined as

$$S(x) := \begin{cases} \max_{c \in \mathcal{Y} \setminus \{y\}} f_c(x) - f_y(x) & \text{(untargeted)} \\ f_{y'}(x) - \max_{c \in \mathcal{Y} \setminus \{y'\}} f_c(x) & \text{(targeted)} \end{cases} \quad (13)$$

where (x, y) is the input-label pair, and the target label is $y' \neq y$. We will estimate gradients of $S(x)$ from $\phi(x) := \text{sign}(S(x))$ which can be obtained from the hard-label query output. This estimator, as used by both HSJA and QEBA, computes a finite difference using uniformly random unit vectors $\{u_b\}_{b=1}^B$, and the corresponding step size α :

$$\nabla_x S(x, \alpha) \approx \frac{1}{B} \sum_{b=1}^B \phi(t(x + \alpha u_b)) u_b \quad (14)$$

Now we rewrite this equation slightly to make it look like we

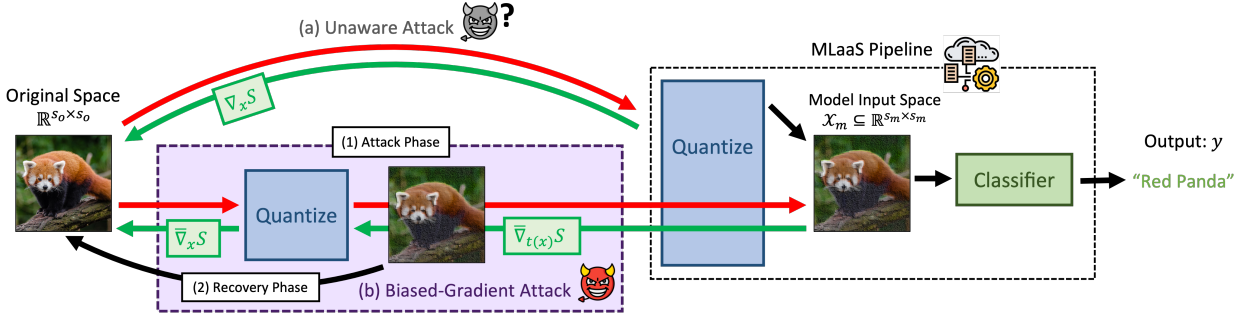


Fig. 5: Simple illustration of Biased-Gradient Attack with quantization as the preprocessor. Biased-Gradient Attack cannot directly operate on the model input space like Bypassing Attack. Rather, it takes advantage of the preprocessor knowledge by modifying a specific attack but still operates in the original space, i.e., the red and the green arrows still go back to the original image.

are estimating gradients w.r.t. $t(x)$ instead of x .

$$\frac{1}{B} \sum_{b=1}^B \phi(t(x + \alpha u_b)) u_b = \frac{1}{B} \sum_{b=1}^B \phi(t(x) + \alpha'_b u'_b) u_b \quad (15)$$

$$\text{where } u'_b = \frac{t(x + \alpha u_b) - t(x)}{\|t(x + \alpha u_b) - t(x)\|_2} \quad (16)$$

$$\text{and } \alpha'_b = \|t(x + \alpha u_b) - t(x)\|_2 \quad (17)$$

Notice that $\alpha'_b u'_b$ represents the random perturbation in the model space. Then, we can roughly “bypass” the preprocessor and approximate gradients in the model space instead by substituting u_b with u'_b in Eqn. (15).

$$\bar{\nabla}_{t(x)} S(x, \alpha) := \frac{1}{B} \sum_{b=1}^B \phi(t(x) + \alpha'_b u'_b) u'_b \quad (18)$$

$$\approx \nabla_{t(x)} S(x, \alpha) \quad (19)$$

So instead of querying the pipeline with $x + \alpha u_b$, we use $t(x + \alpha u_b) = t(x) + \alpha'_b u'_b$ which is equivalent to pre-applying the preprocessor to the queries. Doing so allows us to compute α'_b and u'_b . Note that, due to the idempotence assumption, the model itself sees the same input in both cases. This gradient estimator is biased because u'_b depends on t . Especially, the distribution of u'_b is concentrated around directions that “survive” the preprocessor.

Backpropagate Gradients through Preprocessor This second modification can be used in conjunction with the modification on the gradient approximation step earlier. The new gradient estimate $\bar{\nabla}_{t(x)} S$ can be regarded as gradients w.r.t. the model space, not the original input space where the attack algorithm operates. To account for this, we can backpropagate $\bar{\nabla}_{t(x)} S$ through $t(\cdot)$ according to the chain rule,

$$\bar{\nabla}_x S = \nabla_x t(x) \cdot \bar{\nabla}_{t(x)} S \quad (20)$$

where $\nabla_x t(x)$ is the Jacobian matrix of the preprocessor t w.r.t. the original space. In our experiments, we use the differentiable version of JPEG compression by Shin and Song [30] so the Jacobian matrix exists. For quantization, we approximate $\nabla_x t(x)$ as an identity matrix.

B. Recovery Phase

We propose a recovery phase for general preprocessors which should also work for cropping and resizing as well, albeit less efficiently compared to the one in Bypassing Attack. Assuming that the preprocessor is differentiable or has a differentiable approximation, it is possible to replace the exact projection mechanism for finding x_o^{adv} with an iterative method. Specifically, consider a relaxing the constraint from Eqn. (1) with a Lagrange multiplier:

$$\arg \min_{z_o \in \mathcal{X}_o} \|z_o - x_o\|_2^2 + \lambda \|t(z_o) - x_m^{\text{adv}}\|_2^2. \quad (21)$$

This optimization problem can then be solved with gradient descent combined with a binary search on the Lagrange multiplier λ . We emphasize that unlike the exact recovery for resizing or cropping, the second term does not necessarily need to be driven down to zero, i.e., $t(z_o^*) = x_m^{\text{adv}}$. For the Biased-Gradient Attack, x_m^{adv} can be seen as a proxy to make z_o^* misclassified by $f(t(\cdot))$ or as a guide to move $t(z_o)$ towards. Specifically, we want the smallest λ such that the solution z_o^* minimizes $\|z_o^* - x_o\|_2$ while also being misclassified.

To this end, we use binary search on λ by increasing/decreasing it when z_o^* is correctly/incorrectly classified. Throughout this paper, we use 10 binary search steps, and each step requires exactly one query to check the predicted label at the end. In practice, we also impose a constraint that keeps z_o in the input domain $[0, 1]$ using a change of variable trick inspired by the attack from [7].

Comparing the Bypassing and Biased-Gradient Attacks.

To summarize, there are two major distinctions between Bypassing and Biased-Gradient Attacks:

- 1) The attack phase of Bypassing Attack operates in the model input space directly, while that of the Biased-Gradient Attack is carried out in the original space.
- 2) The Bypassing Attack’s recovery phase is *guaranteed* to yield an adversarial example that is a projection of the original input onto the set that maps to the model-space adversarial example with respect to the Euclidean distance. In other words, the recovered adversarial example is a solution to Eqn. (1). The recovery phase of the Biased-Gradient Attack does not have this guarantee.

TABLE VI: Comparison of the mean adversarial perturbation norm for quantization between the baseline attack unaware of the preprocessor and our Biased-Gradient Attack.

Preprocess	Methods	Hparams	Untargeted		Targeted	
			HSJA	HSJA	QEBA	QEBA
Quantize (8 bits)	Unaware	Default	29.1	83.6	26.5	
		Best	5.0	45.6	26.5	
	Biased-Gradient (ours)	Default	7.1	46.2	21.3	
		Best	3.9	33.9	20.6	
		Change	1.27×	1.35×	1.29×	
Quantize (6 bits)	Unaware	Default	30.4	86.1	40.6	
		Best	7.5	48.2	39.4	
	Biased-Gradient (ours)	Default	11.1	56.7	25.1	
		Best	3.9	34.2	23.3	
		Change	1.92×	1.41×	1.69×	
Quantize (4 bits)	Unaware	Default	32.3	88.9	58.4	
		Best	9.7	63.7	56.4	
	Biased-Gradient (ours)	Default	19.2	74.7	31.8	
		Best	3.2	41.4	30.4	
		Change	3.05×	1.54×	1.86×	

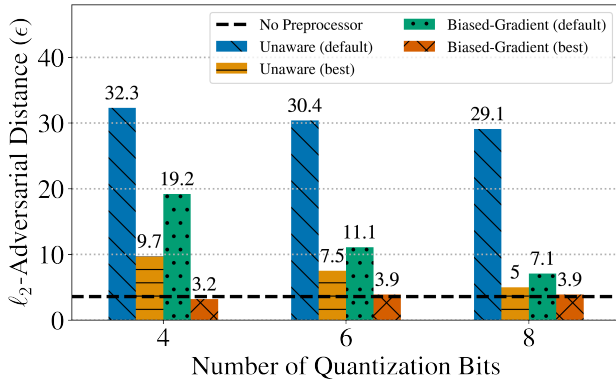


Fig. 6: Visualization showing the improvement on the adversarial distance from the attack hyperparameter tuning (“default”→“best”) and from using the Biased-Gradient Attack instead of the preprocessor-unaware counterpart. We use quantization with varying numbers of bits (4, 6, and 8). The attack algorithm is untargeted HSJA. The dashed line denotes the adversarial distance found by the same attack when no preprocessor is used.

C. Biased-Gradient Attack Results

a) *Quantization*: Quantization is one of the most important preprocessors that the adversary has to overcome since most common image formats such as PNG or JPEG discretize the pixel values. For instance, PNG-8 encodes each pixel with 8 bits which result in the familiar integer values from 0 to 255. Quantization is also important for on-device models where memory and latency are the main deployment constraints. Here, we evaluate our Biased-Gradient Attack on 8-bit, 6-bit, and 4-bit quantization preprocessor (see Table VI).

For all the attack algorithms and all the settings we consider, untargeted/targeted HSJA and targeted QEBA, Biased-Gradient Attack outperforms the preprocessor-unaware counterpart. A general trend is with a stronger preprocessor (fewer bits) the improvement from Biased-Gradient Attack relatively

TABLE VII: Comparison of the mean adversarial perturbation norm for JPEG compression between the baseline attack unaware of the preprocessor and our Biased-Gradient Attack.

Preprocess	Methods	Hparams	Untargeted		Targeted	
			HSJA	HSJA	QEBA	QEBA
JPEG (quality 100)	Unaware	Default	5.7	35.8	18.8	
		Best	3.5	31.9	18.8	
	Biased-Gradient (ours)	Default	28.9	71.9	19.2	
		Best	2.8	32.5	19.2	
		Change	1.23×	0.98×	0.98×	
JPEG (quality 80)	Unaware	Default	29.6	85.7	50.7	
		Best	8.9	63.2	43.9	
	Biased-Gradient (ours)	Default	23.7	80.4	25.5	
		Best	4.1	29.2	24.9	
		Change	2.15×	2.16×	2.29×	
JPEG (quality 60)	Unaware	Default	29.2	86.8	56.1	
		Best	9.2	63.2	52.7	
	Biased-Gradient (ours)	Default	22.2	82.0	27.0	
		Best	2.7	25.1	26.1	
		Change	3.38×	2.51×	2.02×	

increases (the yellow bar vs the orange bar in Fig. 6). This observation is similar to one on the Bypassing Attack with resizing preprocessors of different output sizes. With 4-bit quantization, Biased-Gradient Attack reduces the mean adversarial distance by over 3 times or to only one third of the distance found by the attack without it.

b) *JPEG Compression*: JPEG is a popular image format that compresses images further than a basic quantization operation. JPEG comes with one parameter, an integer between 0 and 100, which indicates the quality of the compressed image where 100 being the highest. In this experiment, we evaluate the attacks with the quality value of 60, 80, and 100, and the results are shown in Table VII. We observe the recurring trend similarly to the earlier preprocessors where the improvement of our Biased-Gradient Attack increases with stronger preprocessors, i.e., lower compression quality.

With quality of 100, JPEG compression is still lossy due to the color sub-sampling step even when no frequency component in the Discrete Fourier Transform space is dropped. With this preprocessor, the Biased-Gradient Attack is beneficial on untargeted HSJA and is slightly outperformed by the baseline for the targeted attacks. However, Biased-Gradient Attack still performs better than the preprocessor-unaware counterpart in every other setting, reducing the mean adversarial distance by a factor between $2\times$ and $3.4\times$.

VII. EXTRACTING PREPROCESSORS

As we have seen, decision-based attacks are incredibly sensitive to the exact preprocessor used, and knowledge of the preprocessor can be used to design much more efficient attacks. Now we develop a query-efficient decision-based extraction attacks to discover what preprocessor is being used by the target system.

It should not be surprising that this task would be achievable as it is a particular instance of the more general problem of model stealing. Specifically, given that recent work has shown a way to completely recover a (functionally-equivalent) neural

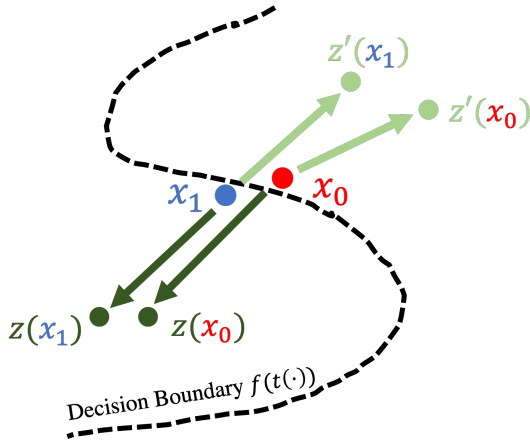


Fig. 7: Diagram of an *unstable example pair*, (x_0, x_1) , where each is predicted as a different class, but when applied with some transformation (either $z(\cdot)$ or $z'(\cdot)$), they are very likely to land on the same side of the decision boundary

network exactly using only query access [6, 22, 28], stealing just a specific part of the model should indeed also be possible.

Nonetheless, there are two factors that make our attack much more difficult than prior model stealing attacks, both of which relate to the assumed adversary’s capabilities:

- 1) Prior functionally-equivalent extraction attacks require the adversary to have *high-precision access* to the classifier. That is, the adversary is able to provide (64-bit) floating point values as input and view the full (64-bit) floating point probability vector as output. However, in our setting, we can only provide valid image files (8 bit) as input and receive only a single decision label as output. This completely invalidates the approaches used in prior work, which require computing finite differences with epsilon-sized input-output perturbations [22].
- 2) Prior functionally-equivalent extraction attacks make hundreds of thousands to tens of millions of queries to extract a very simple (thousand-parameter) MNIST neural networks [6]—in contrast we work over much larger models. While the up-front model stealing cost can be amortized across many generated adversarial examples, for our attacks to be economically efficient, they must be effective in just a few hundred queries.

Intuition. Our extraction attack relies on a *guess-and-check strategy*. Given some hypothesis about the preprocessor (e.g., “the model uses bilinear interpolation to resize the image to 224×224 ”), we build a set of inputs Q such that if the hypothesis is true, then the decision vector $v = \{f(q) : q \in Q\}$ will have one property; otherwise, the decision vector v will be detectably different. Then, by enumerating a space \mathbb{P} of possible preprocessors, we can use a combination of binary search and exhaustive search to reduce this set down to a single preprocessor $p \in \mathbb{P}$ actually being deployed.

A. Unstable Example Pairs

As the first step of our attack, we populate Q with many “unstable example pairs.” An unstable pair is defined as a

pair of samples (x_0, x_1) with two properties: (1) $f(t(x_0)) \neq f(t(x_1))$, but (2) $f(t(z(x_0))) = f(t(z(x_1)))$ with high probability for any transformation $z : \mathcal{X}_o \rightarrow \mathcal{X}_o$. Fig. 7 visually depicts this setting; a transformation z slightly perturbs the example pair so that the two examples no longer perfectly straddle the decision boundary, and now they are both either on the left or the right side (for z') of the boundary.

More formally, because the decision boundary of neural networks are locally linear, they can be approximated by a hyperplane [13]. If we perturb the two examples in any direction other than perfectly parallel to the hyperplane, the decision of at least one of them should change. This probability should only increase as the size of the perturbation made by z (i.e., $z(x) - x$) grows.

Constructing an unstable pair. We begin by identifying (any) two images a, b such that $f(t(a)) \neq f(t(b))$. This step should be easy: it suffices to identify two valid images that actually belong to different classes, or to make random (large-magnitude) modifications to one image a until it switches classes and then call the perturbed image b . Intuitively, because $f(t(a)) \neq f(t(b))$, if we were to interpolate between a and b , there must be a midpoint c where the decision changes. By picking x_0 and x_1 to straddle this midpoint c , we obtain an unstable example pair. If the input space of the pipeline were continuous, we can generate an unstable pair, up to the floating-point precision, with a single binary search. However, since we focus on real systems that accept only 8-bit images, we need to take multiple extra steps to create the pair that differs by only one bit on one pixel.

First, we begin by reducing the ℓ_∞ difference between the two images via binary search. Let $m = (a+b)/2$, and query the model to obtain $f(t(m))$. If $f(t(m)) = f(t(a))$ then replace a with m and repeat; if $f(t(m)) = f(t(b))$ then replace b with m and repeat. Do this until a and b differ from each other by at most $1/255$ (the smallest difference two images can have).

Next, reduce the ℓ_0 difference between these two images, again following the same binary search procedure. Construct a new image m where each pixel is independently chosen (uniformly at random) as the pixel value either from the image a or from the image b . This new image m now roughly shares half of the pixels with a and half of the pixels with b . If $f(t(m)) = f(t(a))$ replace a with m and repeat; and vice versa. This will eventually give a pair of images a, b that now differ in exactly one pixel coordinate, and in this one coordinate by exactly $1/255$. Now we finish our preparation and are ready to begin the guess-and-check attack in Section VII-B. Note that we have not relied on the knowledge of t as we have only treated $f \circ t$ as a single function.

B. Hypothesis Testing with a Second Preimage Attack

Suppose we hypothesize that the first transformation applied to an image is some function \hat{t} (this is our “guess” piece). Then, given this unstable example pair (x_0, x_1) , we can now implement the “check” piece of our guess-and-check attack. For clarity, in this section we denote the actual preprocessor of the deployed model by t^* .

We begin by constructing a *second preimage* $x'_0 \neq x_0$ (via some function A s.t. $x'_0 = A(x_0)$) so that $\hat{t}(x_0) = \hat{t}(x'_0)$

and respectively another example $x'_1 \neq x_1$ so that, similarly, $\tilde{t}(x_1) = \tilde{t}(x'_1)$. Note that A depends on \tilde{t} and so is part of the guess. Now we consider two scenarios where our guess is either right or wrong.

a) *Our guess is correct:* In the case that our guess is right, ($\tilde{t} = t^*$), the following equality will hold for $i \in \{0, 1\}$,

$$f(t^*(x'_i)) = f(\tilde{t}(x'_i)) = f(\tilde{t}(x_i)) = f(t^*(x_i)) \quad (22)$$

where the first equality holds by assumption that $\tilde{t} = t^*$, the second equality holds by construction that x'_i and x_i are second preimages, and the final equality holds under the first correctness assumption. From here, we can conclude

$$\underbrace{f(t^*(x'_0)) = f(t^*(x_0))}_{\text{By Eqn. (22)}} \neq \underbrace{f(t^*(x_1)) = f(t^*(x'_1))}_{\text{By Eqn. (22)}}.$$

Put simply, this means that if we feed the pipeline with x'_0 and x'_1 , and if our preprocessor guess is correct, then the pipeline will give two different answers $f(t^*(x'_0)) \neq f(t^*(x'_1))$.

b) *Our guess is wrong:* On the other hand, if our guess at the preprocessor was wrong, i.e., $\tilde{t} \neq t^*$, then we will, with high probability, observe a different outcome:

$$\underbrace{f(t^*(x'_0)) = f(t^*(A(x_0)))}_{\text{By construction}} \neq \underbrace{f(t^*(A(x_1))) = f(t^*(x'_1))}_{\text{By construction}}$$

where the middle inequality holds true because the examples x_0 and x_1 are an unstable example pair, and A is the non-identity transformation used to construct x'_i from x_i .

By coming up with multiple second preimages, querying the target pipeline, and observing the predictions, we can check whether our guess on the preprocessor is correct or not.

C. A Greedy Second-Preimage Attack

The previous step requires the ability to construct second preimages for an arbitrary image x and an arbitrary guessed transformation \tilde{t} . While in general this problem is intractable (e.g., a cryptographic hash function resists exactly this), common image preprocessors are not explicitly designed to be robust and so in practice, it is often nearly trivial.

In practice, we implement this attack via a greedy and naive attack that works well for any transformation that operates over discrete integers $t : \mathbb{Z}^n \rightarrow \mathbb{Z}^m$, which is the case for image preprocessors where pixel values lie between 0 and 255.

To begin, let a_0 be the image whose second preimage we would like to compute. We then make random pixel-level perturbations to the image a_0 by randomly choosing a pixel coordinate j and either increasing or decreasing its value by $1/255$. We refer to each of these as $\{a_0^j\}_{j=0}^J$. We take each of these candidate a_0^j and check if $\tilde{t}(a_0^j) = \tilde{t}(a_0)$. If any hold true, then we *accept* this change and let $a_1 = a_0^j$. We then repeat this procedure with a_1 to get a sequence of images $a_0, a_1 \dots a_K$ so that $\tilde{t}(a_0) = \dots = \tilde{t}(a_K)$ and that $\|a_0 - a_K\|$ is sufficiently large. We desire large perturbation because, intuitively, the larger the difference, the higher the probability that the unstable property will hold. In other words, it is more

TABLE VIII: Number of queries necessary to determine what preprocessor is being used.

Preprocessor Space	Queries
Arbitrary Resize (200px-1000px)	641
Arbitrary Crop (10%-100%)	140
JPEG Compression Quality (5-100)	464
Typical Preprocessors (see text)	165

likely that $f(t(A(x_0))) = f(t(A(x_1)))$ if $\tilde{t} \neq t$, where x_0 and x_1 are a_K and b_K in this case. In practice we only use one unstable example pair, but if more confidence is desired, an attack could use many (at an increased query cost).

Extracting multiple preprocessors. With the above attack, it becomes trivial to extract multiple preprocessors by extracting each in turn as long as it is possible to compute second preimages through each preprocessor in turn. Suppose there are two preprocessors $t_1(\cdot)$ and $t_2(\cdot)$, we can first extract t_1 by subsuming t_2 as part of f , i.e., $f' \circ t_1 := f \circ t_2 \circ t_1$, and then we move on to guess t_2 using the now revealed t_1 to construct the preimages. Practically, we have found that this is possible for the types of common transformations we study. In practice, it is actually even easier: the most common two transformations, resizing and cropping, are almost commutative (i.e., $\text{crop}(\text{resize}(x)) \approx \text{resize}(\text{crop}(x))$) albeit with different crop and resize parameters). This fact significantly simplifies preprocessor extraction in this common special case.

D. Experimental Results

We implement this attack to extract preprocessors for a range of image models released publicly on the PyTorch Hub and timm repository of image classifiers [38]. Because our procedure is inherently guess-and-check, we must first define the space of all possible preprocessors. The exact space here depends on the possible knowledge an adversary might have.

In the worst case, an adversary might have no knowledge about the image size being used. When this happens we simply enumerate over all possible image sizes ranging from the smallest size used for any image classifier (200×200 pixels) to the largest size used for any image classifier (1000×1000).

In the best case an adversary might be aware of what *typical* preprocessors are in use. For this, we call a preprocessor “typical” if at least two different models use the same setup. For example, ResNet classifiers almost always first resize images to 256×256 , and then center-crop the resulting image down to 224×224 . We find under twenty distinct preprocessors that occur more than once.

VIII. DISCUSSION

A. Varying Number of Attack Iterations

There are two interesting properties we observe when we vary the number of queries the adversary can utilize. So far we have considered attack that use exactly 5,000 queries; in this section we now test attacks with 500 to 50,000 queries. Fig. 8 plots the mean adversarial distance as a function of

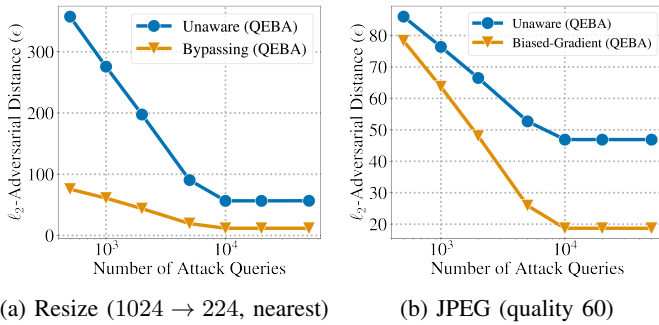


Fig. 8: Mean adversarial distance vs the number of queries used by QEBA on (a) resizing and (b) JPEG compression.

the number of queries for QEBA attack with the best hyperparameter for each respective setting. First, the adversarial distance plateaus after around 10,000 queries, and the distance found by preprocessor-unaware attacks never reaches that of Bypassing/Biased-Gradient Attack. This suggests that our preprocessor-aware attack does not only improve the efficiency of the attack algorithms but also allow it to find closer adversarial examples that would have been completely missed otherwise.

The second observation is that the improvement from Bypassing Attack over the preprocessor-unaware attack is consistent across all numbers of queries. For instance, in Fig. 8a, the Bypassing Attack reduces the mean adversarial distance by a factor of around 4.5 to 4.8 for any number of queries. This is not the case for the Biased-Gradient Attack which is relatively more effective at a larger number of queries. In Fig. 8b, the Biased-Gradient Attack yields an improvement of $1.1\times$ at 500 queries and $2.5\times$ beyond 10,000 queries.

B. Choice of Attack Hyperparameters

We have seen from Section V and VI that fine-tuning the hyperparameters improve the attack significantly in most cases. We discuss when it is most important for the adversary to fine-tune their attack hyperparameters. Fig. 10 (Appendix C) shows the attack success rate at varying adversarial distances for three untargeted attack algorithms. For Boundary, HSJA, and QEBA attacks, the gain from selecting the right set of hyperparameters is significant, a large improvement over the default. **In many cases, using the right hyperparameters benefits more than using stronger attack algorithms.** For instance, a properly tuned Boundary attack outperforms Sign-OPT and HSJA attacks with their default hyperparameters in majority of the settings with resizing preprocessor.

For most attacks, we do not observe a universally good set of hyperparameters across different preprocessors. However, there are two general rules of thumb when it comes to better guess the hyperparameters:

- 1) Using a larger value of γ (10^3 – 10^4) in HSJA attack is almost always better than the default (10). This applies to both preprocessor-aware and -unaware attacks and to all preprocessors.
- 2) QEBA attack samples the noise used for gradient approximation from an image space with a smaller

size $rs_o \times rs_o$ where s_o is the original input size, and r is the hyperparameter smaller than 1. The default value of r is $\frac{1}{4}$ for $s_o = 224$. Consequently, for a larger s_o such as the resizing preprocessor, setting r to be smaller accordingly is always beneficial. For example, we find that for $s_o = 256, 512, 1024$, the best values of r are $\frac{1}{8}, \frac{1}{16}, \frac{1}{32}$, respectively.

C. Multiple Preprocessors

In practice, multiple preprocessors are used sequentially in the input pipeline. As mentioned in Section VII, our extraction method also works in this case by “peeling out” one preprocessor at a time. On the other hand, the attack may depend on the ordering and the specific preprocessors used. We categorizes the combinations into three groups according to the types of the preprocessors.

The first setting is when all the preprocessors can be bypassed, e.g., resizing and cropping. This is a simple case where the attacker can bypass the entire pipeline by querying with an appropriate size and padding. The recovery phase can then be done in the reverse sequence to the order that the preprocessors are applied. The second simple setting is where all the preprocessors are already non-bypassable, e.g., quantization and JPEG compression. Here, all the preprocessors can be combined and treated as one, and the Biased-Gradient Attack can be directly applied as before.

The third is when both types of preprocessors are present. In this setting, we combine the Bypassing and the Biased-Gradient attacks into a single sequential process. For instance, a common pipeline for classifiers trained on the ImageNet dataset consists of 8-bit quantization, resizing to 256×256 , and cropping to 224×224 . To attack this set of preprocessors, we first initialize the attack image by resizing and cropping the original image using the given parameters, which is the same as the normal Bypassing Attack. Next, we run the Biased-Gradient Attack using this initialized image to attack the quantization. Finally, we run the recovery phase for cropping and then resizing as in the first setting.

For this example, our preprocessor-aware attack finds the mean adversarial distance of 40.8 compared to 61.4 of the preprocessor-unaware counterpart, reducing the distance by 34% or $1.5\times$. We use QEBA as the base attack, and the original image size is 512×512 . Note that this special case is only applicable when the bypassable preprocessors are followed by the non-bypassable. Otherwise, we need to resort to the second setting where all the preprocessors have to be combined and treated as one.

IX. CONCLUSION

Adversarial examples have been studied extensively in the academic domain. The existing literature has largely “solved” the problem of evaluating the (white-box) robustness for any given classifier, and while defenses remain imperfect [33], state-of-the-art attack [7] and defense [21] strategies have remained largely unchanged over the past several years.

Despite this, we believe that there are still many underexplored research directions that focus on the *practicality* of generating adversarial examples in real environments. Our paper

takes a first step towards addressing one of these challenges: we have shown that decision-based attacks are not resilient to changes in preprocessors.

The degree to which preprocessors matter is surprising: to develop a strong attack in practice, **it is more important to get the preprocessor right than to use a stronger attack!** That is, we find that a “weak” preprocessor-aware attack performs better than a state-of-the-art attack without knowledge of the preprocessor.

Our observation that preprocessors matter is consistent with observation from recent work that decision-based attacks are exceptionally brittle to (trivial) amounts of randomness applied to the input or the output of a machine learning model [1, 25]. Taken together, these results suggest that there is a large potential for improving current decision-based attacks to work across practical settings. Conversely, if finding such an attack turns out to be hard, then this might suggest that it is easier to defend against adversarial examples in practice than previously thought.

More generally, we believe that it is important for future work to carefully consider other implicit assumptions in the current adversarial machine learning literature that may be not be true in practice. We hope that our analysis will inspire future work to further explore this direction.

ACKNOWLEDGMENT

The authors would like to thank David Wagner for helping with the presentation of the paper, Matthew Jagielski for wonderful discussion on the problem, and Alex Kurakin for comments on early draft of this paper.

REFERENCES

- [1] M. B. Aithal and X. Li, “Mitigating black-box adversarial attacks via output noise perturbation,” *IEEE Access*, vol. 10, pp. 12 395–12 411, 2022.
- [2] A. Athalye, N. Carlini, and D. Wagner, “Obfuscated gradients give a false sense of security: Circumventing defenses to adversarial examples,” in *Proceedings of the 35th International Conference on Machine Learning*, ser. Proceedings of Machine Learning Research, J. Dy and A. Krause, Eds., vol. 80. Stockholm: PMLR, Jul. 2018, pp. 274–283.
- [3] B. Biggio, I. Corona, D. Maiorca, B. Nelson, N. Šrndić, P. Laskov, G. Giacinto, and F. Roli, “Evasion attacks against machine learning at test time,” in *Machine Learning and Knowledge Discovery in Databases*, H. Blockeel, K. Kersting, S. Nijssen, and F. Železný, Eds. Berlin, Heidelberg: Springer Berlin Heidelberg, 2013, pp. 387–402.
- [4] W. Brendel, J. Rauber, and M. Bethge, “Decision-based adversarial attacks: Reliable attacks against black-box machine learning models,” in *International Conference on Learning Representations*, 2018.
- [5] W. Brendel, J. Rauber, A. Kurakin, N. Papernot, B. Velicki, M. Salathé, S. P. Mohanty, and M. Bethge, “Adversarial vision challenge,” Tech. Rep., 2018.
- [6] N. Carlini, M. Jagielski, and I. Mironov, “Cryptanalytic extraction of neural network models,” in *Annual International Cryptology Conference*. Springer, 2020, pp. 189–218.
- [7] N. Carlini and D. Wagner, “Towards evaluating the robustness of neural networks,” in *2017 IEEE Symposium on Security and Privacy (SP)*, 2017, pp. 39–57.
- [8] J. Chen, M. I. Jordan, and M. J. Wainwright, “Hop-SkipJumpAttack: A query-efficient decision-based attack,” *arXiv:1904.02144 [cs, math, stat]*, Apr. 2020.
- [9] P.-Y. Chen, H. Zhang, Y. Sharma, J. Yi, and C.-J. Hsieh, “ZOO: Zeroth order optimization based black-box attacks to deep neural networks without training substitute models,” in *Proceedings of the 10th ACM Workshop on Artificial Intelligence and Security*, ser. AISec ’17. New York, NY, USA: Association for Computing Machinery, 2017, pp. 15–26.
- [10] M. Cheng, S. Singh, P. H. Chen, P.-Y. Chen, S. Liu, and C.-J. Hsieh, “Sign-OPT: A query-efficient hard-label adversarial attack,” in *International Conference on Learning Representations*, 2020.
- [11] Clarifai, “Best NSFW model for content detection using AI — clarifai,” <https://www.clarifai.com/models/nsfw-model-for-content-detection>.
- [12] J. Deng, W. Dong, R. Socher, L.-J. Li, K. Li, and L. Fei-Fei, “ImageNet: A large-scale hierarchical image database,” in *2009 IEEE Conference on Computer Vision and Pattern Recognition*, 2009, pp. 248–255.
- [13] I. Goodfellow, J. Shlens, and C. Szegedy, “Explaining and harnessing adversarial examples,” in *International Conference on Learning Representations*, 2015.
- [14] C. Guo, J. Gardner, Y. You, A. G. Wilson, and K. Weinberger, “Simple black-box adversarial attacks,” in *Proceedings of the 36th International Conference on Machine Learning*, ser. Proceedings of Machine Learning Research, K. Chaudhuri and R. Salakhutdinov, Eds., vol. 97. PMLR, Jun. 2019, pp. 2484–2493.
- [15] C. Guo, M. Rana, M. Cisse, and L. van der Maaten, “Countering adversarial images using input transformations,” in *International Conference on Learning Representations*, 2018.
- [16] K. He, X. Zhang, S. Ren, and J. Sun, “Deep residual learning for image recognition,” in *2016 IEEE Conference on Computer Vision and Pattern Recognition (CVPR)*, 2016, pp. 770–778.
- [17] A. Ilyas, L. Engstrom, A. Athalye, and J. Lin, “Black-box adversarial attacks with limited queries and information,” in

- Proceedings of the 35th International Conference on Machine Learning*, ser. Proceedings of Machine Learning Research, J. Dy and A. Krause, Eds., vol. 80. PMLR, Jul. 2018, pp. 2137–2146.
- [18] M. Jagielski, N. Carlini, D. Berthelot, A. Kurakin, and N. Papernot, “High accuracy and high fidelity extraction of neural networks,” in *29th USENIX Security Symposium (USENIX Security 20)*. USENIX Association, Aug. 2020, pp. 1345–1362.
- [19] A. Jha and R. Mamidi, “When does a compliment become sexist? analysis and classification of ambivalent sexism using twitter data,” in *Proceedings of the Second Workshop on NLP and Computational Social Science*. Vancouver, Canada: Association for Computational Linguistics, Aug. 2017, pp. 7–16. [Online]. Available: <https://aclanthology.org/W17-2902>
- [20] H. Li, X. Xu, X. Zhang, S. Yang, and B. Li, “QEBA: Query-efficient boundary-based blackbox attack,” in *Proceedings of the IEEE/CVF Conference on Computer Vision and Pattern Recognition (CVPR)*, Jun. 2020.
- [21] A. Madry, A. Makelov, L. Schmidt, D. Tsipras, and A. Vladu, “Towards deep learning models resistant to adversarial attacks,” in *International Conference on Learning Representations*, 2018.
- [22] S. Milli, L. Schmidt, A. D. Dragan, and M. Hardt, “Model reconstruction from model explanations,” in *Proceedings of the Conference on Fairness, Accountability, and Transparency*, 2019, pp. 1–9.
- [23] N. Papernot, P. McDaniel, I. Goodfellow, S. Jha, Z. B. Celik, and A. Swami, “Practical black-box attacks against machine learning,” in *Proceedings of the 2017 ACM on Asia Conference on Computer and Communications Security*, ser. ASIA CCS ’17. New York, NY, USA: Association for Computing Machinery, 2017, pp. 506–519.
- [24] F. Pierazzi, F. Pendlebury, J. Cortellazzi, and L. Cavallaro, “Intriguing properties of adversarial ML attacks in the problem space,” in *2020 IEEE Symposium on Security and Privacy (SP)*, May 2020, pp. 1332–1349.
- [25] Z. Qin, Y. Fan, H. Zha, and B. Wu, “Random noise defense against query-based black-box attacks,” *Advances in Neural Information Processing Systems*, vol. 34, pp. 7650–7663, 2021.
- [26] E. Quiring, D. Klein, D. Arp, M. Johns, and K. Rieck, “Adversarial preprocessing: Understanding and preventing image-scaling attacks in machine learning,” in *29th USENIX Security Symposium (USENIX Security 20)*. USENIX Association, Aug. 2020, pp. 1363–1380.
- [27] J. Rauber, W. Brendel, and M. Bethge, “Foolbox: A python toolbox to benchmark the robustness of machine learning models,” *arXiv preprint arXiv:1707.04131*, 2017.
- [28] D. Rolnick and K. Kording, “Reverse-engineering deep relu networks,” in *International Conference on Machine Learning*. PMLR, 2020, pp. 8178–8187.
- [29] A. Shafahi, W. R. Huang, C. Studer, S. Feizi, and T. Goldstein, “Are adversarial examples inevitable?” in *International Conference on Learning Representations*, 2019.
- [30] R. Shin and D. Song, “JPEG-resistant adversarial images,” in *Machine Learning and Computer Security Workshop (Co-Located with NeurIPS 2017)*, Long Beach, CA, USA, 2017.
- [31] Y. Song, T. Kim, S. Nowozin, S. Ermon, and N. Kushman, “PixelDefend: Leveraging generative models to understand and defend against adversarial examples,” *arXiv:1710.10766 [cs]*, May 2018.
- [32] C. Szegedy, W. Zaremba, I. Sutskever, J. Bruna, D. Erhan, I. Goodfellow, and R. Fergus, “Intriguing properties of neural networks,” in *International Conference on Learning Representations*, 2014.
- [33] F. Tramer, N. Carlini, W. Brendel, and A. Madry, “On adaptive attacks to adversarial example defenses,” in *Advances in Neural Information Processing Systems*, H. Larochelle, M. Ranzato, R. Hadsell, M. F. Balcan, and H. Lin, Eds., vol. 33. Curran Associates, Inc., 2020, pp. 1633–1645.
- [34] F. Tramèr, P. Dupré, G. Rusak, G. Pellegrino, and D. Boneh, “Adversarial: Perceptual ad blocking meets adversarial machine learning,” in *Proceedings of the 2019 ACM SIGSAC Conference on Computer and Communications Security*, Nov. 2019, pp. 2005–2021.
- [35] F. Tramèr, F. Zhang, A. Juels, M. K. Reiter, and T. Ristenpart, “Stealing machine learning models via prediction APIs,” in *Proceedings of the 25th USENIX Conference on Security Symposium*, ser. SEC’16. USA: USENIX Association, 2016, pp. 601–618.
- [36] C.-C. Tu, P. Ting, P.-Y. Chen, S. Liu, H. Zhang, J. Yi, C.-J. Hsieh, and S.-M. Cheng, “AutoZOOM: Autoencoder-based zeroth order optimization method for attacking black-box neural networks,” *arXiv:1805.11770 [cs, stat]*, Jan. 2020.
- [37] Z. Waseem, T. Davidson, D. Warmsley, and I. Weber, “Understanding abuse: A typology of abusive language detection subtasks,” in *Proceedings of the First Workshop on Abusive Language Online*. Vancouver, BC, Canada: Association for Computational Linguistics, Aug. 2017, pp. 78–84. [Online]. Available: <https://aclanthology.org/W17-3012>
- [38] R. Wightman, “PyTorch image models,” GitHub, 2019.

A. Hyperparameter Sweep

For Boundary attack, we sweep the two choices of step size, one along the direction towards the original input and the other in the orthogonal direction. The default values are (0.01, 0.01), respectively, and the swept values are (0.1, 0.01), (0.001, 0.01), (0.01, 0.1), and (0.01, 0.001).

For Sign-OPT attack, we consider the update step size α and the gradient estimate step size β . Their default values are (0.2, 0.001) respectively, and we sweep the following values: (0.2, 0.01), (0.2, 0.0001), (0.02, 0.001), and (2, 0.01).

We only tune one hyperparameter for HSJA and QEBA attacks but with the same number of settings (five) as the other two attacks above. For HSJA, we tune the update step size γ by trying values of 10^1 (default), 10^2 , 10^3 , 10^4 , and 10^5 . Optimal value of γ is always at a higher range than 10^1 , not smaller. Lastly, we search the ratio r that controls the latent dimension that QEBA samples its random noise from for gradient approximation. We search over $r = 2, 4, 8, 16, 32$.

B. Formal Definition of Cropping’s Recovery Phase

We now formally describe what it means to crop an image. Given an input image of size $s_o \times s_o$, a crop operation removes the edge pixels of any image larger than a specified size, denoted by $s_m \times s_m$, such that the output has the size $s_o \times s_o$. Given an (flattened) input image $x_o \in \mathbb{R}^{s_o \times s_o}$ and the cropped image $x_m \in \mathbb{R}^{s_m \times s_m}$, we can write cropping as the following linear transformation, when $s_o > s_m$,

$$x_m = M^{\text{crop}} x_o \quad (23)$$

where $M^{\text{crop}} \in \mathbb{R}^{s_o^2 \times s_m^2}$ is a sparse binary matrix. Each row of M^{crop} has exactly one entry being 1 at a position of the corresponding non-edge pixel while the rest are 0. Note that we drop the “color-channel” dimension for simplicity since most of the preprocessors in this paper is applied channel-wise. We are only interested in the scenario when $s_o > s_m$ because otherwise, the preprocessing simply becomes an identity function.

Let the adversarial example in the model space as obtained from the attack phase be $x_m^{\text{adv}} \in \mathbb{R}^{s_m \times s_m}$. The adversary can recover the corresponding adversarial example in the original space, $x_o^{\text{adv}} \in \mathbb{R}^{s_o \times s_o}$, by padding x_m^{adv} with the edge pixels of x_o .

It is simple to show that x_o^{adv} is a projection of x_o onto the set $\mathcal{T}^{\text{crop}}(x_m^{\text{adv}}) := \{x \in \mathcal{X}_o \mid t^{\text{crop}}(x) = x_m^{\text{adv}}\}$, i.e.,

$$x_o^{\text{adv}} = \arg \min_{x \in \mathcal{T}^{\text{crop}}(x_m^{\text{adv}})} \|x - x_o\|_2^2 \quad (24)$$

Proof: We can split $\|x - x_o\|_2^2$ into two terms

$$\sum_{i \in E} ([x]_i - [x_o]_i)^2 + \sum_{i \notin E} ([x]_i - [x_o]_i)^2 \quad (25)$$

where E is a set of edge pixel indices. The second term is fixed to $\|x_m^{\text{adv}} - t^{\text{crop}}(x_o)\|_2^2$ for any $x \in \mathcal{T}^{\text{crop}}(x_m^{\text{adv}})$. When $x = x_o^{\text{adv}}$, the first term is zero because x_o^{adv} is obtained by padding x_m^{adv} with the edge pixels of x_o . Since the first term is non-negative, we know that x_o^{adv} is a unique global minimum of Eqn. (24). ■

C. Additional Experiment Results

Here, we include two figures that compare the effect of tuning the attack hyperparameters in multiple settings. Fig. 9 suggests that the default hyperparameters often work well as expected when no preprocessor is used while there is much greater discrepancy between the default and the best hyperparameters when preprocessors are used.

The degree in which the hyperparameter tuning matters also depends on the attack algorithm. Fig. 10 visually compares the effectiveness of three untargeted attacks on the resizing preprocessor. It is obvious that Boundary and HSJA attacks benefit much more from a hyperparameter sweep compared to Sign-OPT attack.

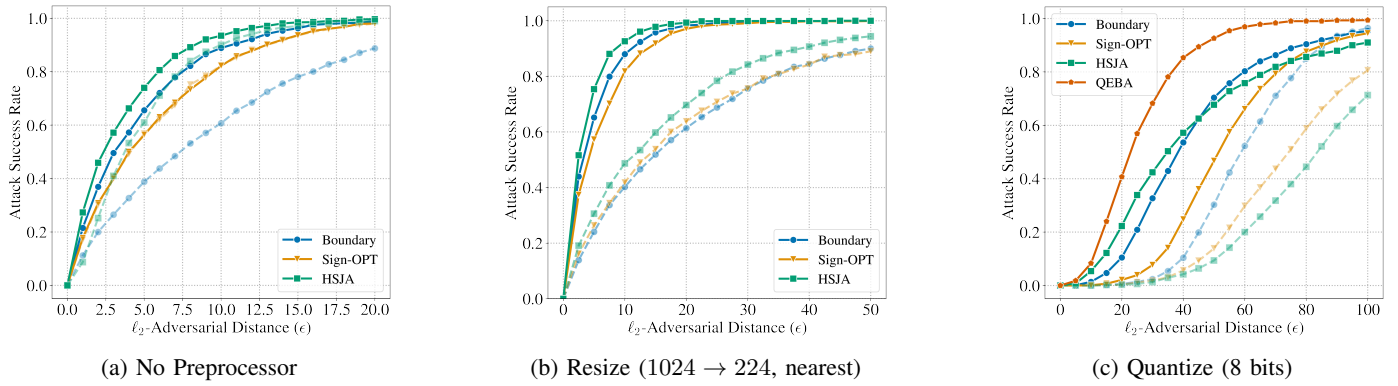


Fig. 9: Plots of the attack success rate at varying maximum adversarial distance with different preprocessors. The darker solid lines denote the preprocessor-unaware and the Bypassing attacks with their respectively best hyperparameters. The dashed lines denote the default hyperparameters, and the remaining lighter solid lines correspond to the other set of hyperparameters we sweep.

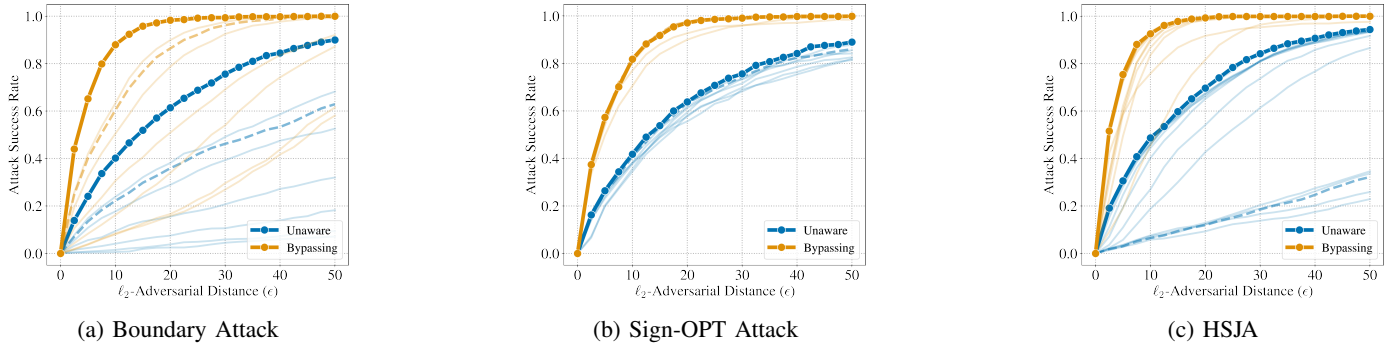


Fig. 10: Plots of the attack success rate at varying maximum adversarial distance. Here, the preprocessor is resizing with nearest interpolation from 1024×1024 to 224×224 , corresponding to the first five rows of Table III (untargeted). The solid lines with markers denote the preprocessor-unaware and the Bypassing attacks with their respectively best hyperparameters. The dashed lines denote the default hyperparameters, and the remaining lighter solid lines correspond to the other set of hyperparameters we sweep.